

RESEARCH

Open Access



# Genome-wide identification and comparative evolution of 14–3–3 gene family members in five Brassicaceae species

Jingya Zhao<sup>1,2†</sup>, Shengqin Liu<sup>1,2†</sup>, Hui Ren<sup>1,2</sup>, Owusu Edwin Afriyie<sup>2</sup>, Mengzhu Zhang<sup>2</sup>, Dachao Xu<sup>2</sup> and Xianzhong Huang<sup>2\*</sup>

## Abstract

**Background** The 14–3–3 proteins are highly conserved regulatory eukaryotic proteins, which are crucial in growth, development, and stress responses. However, systematic characterization of the 14–3–3 gene family in Brassicaceae species and their evolutionary relationships have not been comprehensively reported.

**Results** This study conducted genome-wide identification, structural characteristics, and comparative evolutionary analysis of 14–3–3 gene family members in *Arabidopsis thaliana*, *A. lyrata*, *A. pumila*, *Camelina sativa*, and *Brassica oleracea* using comparative genomics. Overall, a total of 108 14–3–3 genes, which were phylogenetically classified into  $\epsilon$  and non- $\epsilon$  groups were identified in the five species, with the non- $\epsilon$  members exhibiting more similar exon–intron structures and conserved motif patterns. Collinearity analysis revealed that the Brassicaceae 14–3–3 gene family members underwent varying degrees of expansion following whole-genome duplication (WGD) events. Notably, the number of 14–3–3 gene family members between *A. lyrata* and *A. thaliana* remained similar despite the former having approximately 1.66-fold larger genome size. In contrast, the number of 14–3–3 gene family members in *A. pumila* and *C. sativa* increased in proportionately to their genome size, while gene members in the more distantly related species to *A. thaliana*, *B. oleracea*, showed irregular expansion patterns. Selection pressure analysis revealed that 14–3–3 homologs in all the five species underwent purifying selection, with the group  $\epsilon$  members experiencing relatively weaker purifying selection. Cloning of *ApGRF6-2* gene from *A. pumila* indicated that the ApGRF6-2 protein was localized in the cell membrane and cytoplasm, while ectopic overexpression of *ApGRF6-2* in *A. thaliana* could promote early flowering by upregulating the expression of floral meristem identity genes.

**Conclusion** This study provides a comprehensive and systematic identification of the 14–3–3 gene family members in five Brassicaceae species using updated genome sequences, and the results could form a basis for further validation of functional and molecular mechanisms of 14–3–3 genes in plant growth, development, abiotic stress responses, as well as flowering regulation.

**Keywords** 14–3–3 gene family, *Arabidopsis pumila*, Evolution, Flowering, Abiotic Stress

<sup>†</sup>Jingya Zhao and Shengqin Liu contributed equally to this work.

\*Correspondence:

Xianzhong Huang  
huangxz@ahstu.edu.cn

<sup>1</sup> College of Life Sciences, Shihezi University, Shihezi 832003, China

<sup>2</sup> Center for Crop Biotechnology, College of Agriculture, Anhui Science and Technology University, Chuzhou 233100, China

## Introduction

The 14–3–3 protein family contains highly conserved acidic and water-soluble proteins that are ubiquitously distributed in eukaryotes. The family was initially identified in bovine brain tissue and functionally crucial regulators of cellular life activities and plant growth and development [1]. The plant 14–3–3 proteins are



composed of two monomers that form homo- or heterodimers and are considered part of the G-box protein complex, thus, they are also referred to as the G-box Factor 14–3–3 homologs (GF14) or General Regulatory Factors (GRF) [2, 3].

The 14–3–3 proteins in plants function as adaptor/scaffold proteins, interacting with target proteins to modulate their activity, dephosphorylation, subcellular localization, and expression [4–6]. Based on their sequence homology and introns count, the 14–3–3 gene family can be divided into  $\epsilon$  and non- $\epsilon$  subfamilies. The  $\epsilon$  subfamily typically contains more introns, while the non- $\epsilon$  members exhibit stronger H<sup>+</sup>-ATPase binding and activation [7]. Structurally, the highly conserved 14–3–3 proteins are generally categorized into three regions, including the variable N-terminal, the conserved core region, and the multifunctional C-terminal, with the pSer or pThr that interacts with target proteins typically located within the polar groove of the conserved core region [8, 9]. Moreover, 14–3–3 proteins can form dimers at the N-terminal site, while the C-terminal interacts with target proteins [10]. The motifs within target proteins that interact with 14–3–3 proteins are mainly categorized into three distinct types: motif I (R/K)SX(S/T)PXP, motif II (R/R)X $\Phi$ X(S/T)PXP (with  $\Phi$  indicating an aromatic or aliphatic amino acid and X representing any amino acid) [11, 12], and the C-terminal motif III (S/T)P X 1–2–COOH [13, 14]. Motif I and II are the main modes that recognize 14–3–3 proteins, while motif III exhibits a relatively weaker binding affinity [15].

Recent years have witnessed increased identification of the 14–3–3 gene family members in several species, including rice (*Oryza sativa*) [16], grape vine (*Vitis vinifera*) [17], cotton (*Gossypium hirsutum*) [18], potato (*Solanum tuberosum*) [19], and tobacco (*Nicotiana tabacum*) [20]. Numerous studies have shown that 14–3–3 proteins can form complexes with their interacting proteins to regulate various aspects of plant growth and development. For example, 14–3–3 acts as a receptor for the florigen FLOWERING LOCUS T (FT) in the shoot apical meristem (SAM). The resulting complex is transported to the nucleus where it binds with the bZIP transcription factor FD to form the florigen activation complex (FAC) that regulates the transition to flowering [21, 22]. In potato, 14–3–3/74 protein interacts with SELF-PRUNING protein (a homolog of *A. thaliana* TERMINAL FLOWER1), and overexpression of the 14–3–3/74 gene can rescue for the loss of *SELF-PRUNING* function [23]. Moreover, complexes formed by 14–3–3 and its interacting proteins exhibit significant regulatory roles in plant responses to abiotic stresses, including drought, salt, cold, and heat. For example, transgenic *Arabidopsis* plants overexpressing *At14-3-3 $\lambda$*  exhibited reduced cold

tolerance [24]. Moreover, proteomic studies on *Brassica napus* have shown that 14–3–3 proteins participate in the responses to salt and drought stresses [25].

The Brassicaceae family, as one of the largest and most diverse group of flowering plants that harbors a critical position in plant systematics and evolutionary studies [26]. WGD events are the major driving force behind the evolution and diversification of Brassicaceae species. During gene evolution, redundant genes following WGD can evolve new functions through sub-functionalization and neofunctionalization to enhance plant adaptability to the environment. Similarly, WGD can also trigger reconstruction of gene expression regulatory networks, which can modify various aspects of plant growth, development, metabolic pathways, and stress responses [27, 28]. *A. thaliana* has undergone at least five WGD events [29], which provides a genetic basis for its adaptability and diversity, while *A. lyrata* has experienced a WGD event common to all Brassicaceae species (At- $\alpha$ ), which has significantly modified its genome evolution and adaptability [30]. In contrast, Brassica plants experienced additional whole-genome triplication event (Br- $\beta$ ) approximately 17 million years ago, which through increased gene dosage, enhanced recombination, and polyploidy effects, contributed to a broader ecological niche distribution in these crops [31]. Moreover, an allopolyploid, *C. sativa* plant has also undergone an additional whole-genome triplication event [32], which not only shaped its genomic features, but also had potential significant implications for its physiology, ecology, and evolution.

Since the first release of *A. thaliana* genome sequence approximately 25 years ago [33], the genomes of nearly 1,500 plant species have subsequently been sequenced, with the genome sequences of species [34], such as *A. lyrata* [35], *C. sativa* [32], and *B. oleracea* [36] having also been completed. Comparative genomics studies indicate that the genome of *A. lyrata* (207 Mb) is approximately 1.66 times the size of that of *A. thaliana* (125 Mb) [35], while the genome size of the allopolyploid *C. sativa* is about three times the size of *A. thaliana* [32]. Interestingly, *B. oleracea* genome has been shown to have high degree of collinearity with the *A. thaliana* genome [36, 37]. *A. pumila* is a salt tolerant ephemeral plant in the Brassicaceae family with a relatively recent WGD that primarily occurs in the deserts of Xinjiang, China [38–41]. Although the 14–3–3 genes have been reported in numerous plant species, reaches on the identification, structural characterization, and comparative evolution of this gene family in Brassicaceae species using recently updated genome sequences remain limited.

Here, bioinformatic techniques were used to systematically identify the 14–3–3 gene family members, perform structural analysis of gene and protein domain features,

as well as their evolutionary relationships from the complete genomes of five Brassicaceae species. In addition, the expression profiles of *A. pumila* 14–3–3 gene members in different tissues in response to salt stress as well as the role of *ApGRF6-2* in the regulation of flowering transition were analyzed. Our results provide a foundation for further systematic analysis of the evolutionary history of the Brassicaceae 14–3–3 gene family, evaluation of their functional roles and molecular mechanisms in environmental adaptation, and prediction of species-specific functional genes.

## Materials and methods

### Plant materials

The seeds of wild-type *A. thaliana* (Col-0) and *A. pumila* were sterilized and cultured on 1/2 Murashige and Skoog (MS) medium for about 7 days at 23°C in darkness [42]. Afterward, the seedlings were transferred to a plant growth room under long-day (LD) conditions (16 h light/8 h dark, 23 °C, 200  $\mu\text{mol m}^{-2} \text{s}^{-1}$ ) for further growth. Samples were collected from various developmental stages of *A. pumila*: hypocotyls (8 d), cotyledons (8 d), roots (30 d), stems (30 d), rosette leaves (30 d), flowers (65 d), and pods (70 d). Four-week-old *A. pumila* plants were watered with 1/2 MS nutrient mixture supplemented with 250 mM NaCl as described previously [39]. Leaf tissues were collected at 7 different time points (0, 0.5, 3, 6, 12, 24, and 48 h) after stress treatment. Col-0 and transgenic *A. thaliana* SAM samples were collected at the stage of third true leaf expansion. All the collected materials were quickly frozen in liquid nitrogen and stored at  $-80$  °C for subsequent gene expression analysis. Each treatment was conducted in three biological replicates.

### Identification of 14–3–3 genes in Brassicaceae species

The genome data for *A. lyrata* [35], *C. sativa* [32], and *B. oleracea* [36] were downloaded from the Ensembl Plants genome database (<https://plants.ensembl.org>); while the *A. thaliana* genome data (TAIR10.1) was obtained from the *A. thaliana* Information Resource website (TAIR, <https://www.arabidopsis.org>). The *A. pumila* genome data were provided by our laboratory. The protein sequences of the *A. thaliana* 14–3–3 gene family were used as queries to perform BLASTP searches against the protein sequence databases of *A. lyrata*, *A. pumila*, *C. sativa*, and *B. oleracea*, with an *E*-value  $\leq 1e^{-10}$ . The retrieved protein sequences were then submitted to the PfamScan website (<https://www.ebi.ac.uk/jdispatcher/pfa/pfamscan>) for domain alignment. Genes corresponding to protein sequences containing the 14–3–3 protein domain (PF00244) were considered members of the 14–3–3 gene family in each species. The naming of genes was

based on their similarity to *A. thaliana* 14–3–3 homologs and their gene structure features (Table S1). The molecular weight, isoelectric point, and grand average hydrophobicity (GRAVY) were estimated using the ExPASy (<https://web.expasy.org/protparam/>) protein analysis tool. Subcellular localization information was predicted using Plant-mPLoc (<http://www.csbio.sjtu.edu.cn/bioinf/plant-multi/>).

### Sequence alignment and phylogenetic analysis

The amino acid conservation of 14–3–3 protein sequences in five Brassicaceae species was analyzed with DNAMAN software. All acquired sequences were first aligned using ClustalX software [43] with the default parameters. An unrooted neighbor-joining (NJ) phylogenetic tree was constructed using MEGA11 [44] software with 1000 bootstrap replicates.

### Gene structure and conserved motif analysis

Gene structure information of 14–3–3 genes in each species was extracted using the TBtools-II software [45] based on the genome gff files of the five species. The exon–intron distribution of the 14–3–3 genes was analyzed using the Gene Structure Display Server (GSDS, <http://gsds.cbi.pku.edu.cn/>). Conserved motifs in the 14–3–3 proteins from each species were identified using the MEME website (<http://meme-suite.org/tools/meme>), with motif lengths ranging from 10 to 60 amino acid residues and a maximum of 10 motifs. Other parameters were set to default values.

### Collinearity analysis, selection pressure, and duplication of the 14–3–3 gene family

The inter- and intra-species collinearity of 14–3–3 genes among *A. thaliana* and the other four Brassicaceae species was defined using the MCScanX method within TBtools-II software [45, 46]. The nonsynonymous substitution rate (*K*<sub>a</sub>) and synonymous substitution rate (*K*<sub>s</sub>) were calculated using DnaSP 6.0 software [47]. Selective pressure on the 14–3–3 genes during evolution was assessed by analyzing the *K*<sub>a</sub>/*K*<sub>s</sub> ratios of collinear gene pairs of the 14–3–3 gene family in the five species of Brassicaceae. A *K*<sub>a</sub>/*K*<sub>s</sub> ratio  $> 1$ ,  $< 1$ , or  $= 1$  indicates positive, negative, or neutral selection, respectively [48]. Potential segmental duplication and tandem duplication events were investigated using TBtools-II software [45].

### Analysis of cis-acting elements in the promoters of 14–3–3 genes

The 2000 bp DNA region upstream of the start codon (ATG) of the 14–3–3 genes was extracted from the genomes of the five species. The presumed promoter regions of each 14–3–3 gene were then submitted to

Plant CARE (<https://bioinformatics.psb.ugent.be/webtools/plantcare/html/>) for analysis of *cis*-acting elements in the promoters. *Cis*-acting elements were visualized in the promoter regions using TBtools-II software [45].

#### Expression profile analysis of *A. pumila* 14–3–3 genes using RNA-seq data

RNA-seq data for seven tissues (cotyledons, hypocotyls, stems, rosette leaves, roots, flowers, and siliques) of *A. pumila* and leaf tissues under 250 mM NaCl stress at seven different time points (0, 0.5, 3, 6, 12, 24, and 48 h) were obtained from the SRA database (<https://www.ncbi.nlm.nih.gov/sra>) (Tables S2 and S3) [39]. The RNA-seq data were standardized using Cufflinks software [49]. The fragments per kilobase per million reads (FPKM) values were log-transformed using Log2 (FPKM + 1), and the results were visualized with heatmaps using TBtools-II software [45].

#### Total RNA extraction and expression analysis of *Ap14-3-3* genes

Specific primers for the *Ap14-3-3* gene were designed using Primer 3.0 (<https://primer3.ut.ee/>) (Table S4), and the *ApGAPDH* gene was used as the internal control for normalizing gene expression in real-time quantitative reverse transcription PCR (qRT-PCR) analysis [50]. Total RNA from each sample was extracted using the RNAPrep Pure Plant Plus Kit (TianGen, China) according to the manufacturer's protocol, and cDNA was synthesized using the MonScript™ RTIII All-in-One Mix with dsDNase kit (Monad, Wuhan) as directed by the manufacturer. The qRT-PCR experiment was performed on an ABI ViiA7 Real-Time PCR System (Life Technologies, USA). The qRT-PCR system and methods used were as described by Jin et al. [50]. The relative expression levels of genes in different tissues were calculated using the 2<sup>-ΔΔC(T)</sup> method, and the relative expression levels of genes under salt stress at different time points were calculated using the 2<sup>-ΔΔΔC(T)</sup> method [51]. For each sample, three biological repeats, with three technical replicates each, were performed to assess the reliability of the results. The results are presented as mean ± standard deviation (SD). All statistical analyses were conducted using Duncan multiple-range test, and different letters were used to denote significant differences ( $P < 0.05$ ).

#### Prediction of 3D structure and subcellular localization analysis

Based on the amino acid sequences of *GRF6* homologous genes from five species of Brassicaceae, the initial models of the *GRF6* proteins from these five species were predicted using AlphaFold 3 [52]. The 3D structures were

then visualized using ChimeraX [53]. Based on the coding sequence (CDS) of the *ApGRF6-2* gene, primers without the stop codon were designed (Table S4). The target fragment was amplified by PCR, and a 35S:*ApGRF6-2*-GFP green fluorescent protein (GFP) fusion overexpression vector was constructed following the method described by Guo et al. [54]. The *ApGRF6-2* coding sequence, excluding the stop codon, was cloned and inserted into the pEASY-Blunt-Zero (TRAN, Beijing) vector and transformed into *Escherichia coli* DH5α. Using T<sub>4</sub> ligase, the correctly sequenced gene fragment was ligated with the pCAMBIA2300-GFP vector [54] and transformed into *E. coli* DH5α. The correct plasmid, 35S:*ApGRF6-2*, was then transformed into *Agrobacterium* GV3101. The *A. thaliana* protoplast subcellular localization experiment was conducted as described by Liu et al. [55].

#### Genetic transformation of *A. thaliana*

The 35S:*ApGRF6-2* construct was created by inserting the *ApGRF6-2* CDS downstream of the Cauliflower mosaic virus (CaMV) 35S promoter into the binary vector pCAMBIA2300-OCS [54]. The recombinant plasmid 35S:*ApGRF6-2* was introduced into *Agrobacterium* GV3101, and then transformed into wild-type *A. thaliana* (Col-0) using the floral dip method [56]. Transgenic *A. thaliana* positive plants were selected on 1/2 MS medium containing 50 mg/ml kanamycin, and homozygous 35S:*ApGRF6-2* transgenic lines were obtained. Under LD conditions, the flowering time and the number of rosette leaves at flowering were observed and counted for Col-0 and two homozygous 35S:*ApGRF6-2* transgenic lines. The expression levels of *ApGRF6-2* and flowering-related genes in the SAM of Col-0 and the two homozygous 35S:*ApGRF6-2* transgenic *A. thaliana* lines were measured by qRT-PCR, with *AtActin2* (GenBank accession no. NM\_180280) used as the internal reference gene (Table S4).

## Results

### Identification and comparative evolution of 14–3–3 gene family members in five Brassicaceae species

Analysis of the whole-genome sequences revealed a total of 13, 24, 39, and 19 14–3–3 gene members in *A. lyrata*, *A. pumila*, *C. sativa*, and *B. oleracea*, respectively (Table S1). Cumulatively, the five plant species contained 108 genes, with *A. thaliana* and *A. lyrata* having the fewest 14–3–3 genes (both with 13 genes), while *C. sativa* had most 14–3–3 genes, with 39 members. The proteins encoded by the 14–3–3 genes showed amino acid (aa) sequence length ranging from 166 (CsGRF3-5) to 413 (CsGRF12-2) aa, molecular weights ranging from 18.36 (CsGRF3-5) to 47.51 (CsGRF12-2) kDa, and isoelectric points (pI) ranging from 4.47 (AtGRF7) to 5.49 (AlGRF13). All proteins

were found to be acidic, while the GRAVY for all 14–3–3 proteins was less than zero, indicating that all members were hydrophilic. Subcellular localization prediction showed that 14–3–3 proteins from the five species were primarily localized in the nucleus, with some members showing dual localization in both the nucleus and the cytoplasm (Table S1).

Evolutionary analysis of the 14–3–3 gene family members in Brassicaceae species using multiple alignment of the amino acid sequences showed that the secondary structures of the 108 14–3–3 proteins contained 9  $\alpha$ -helices, with  $\alpha$ 3 and  $\alpha$ 4 as the longest helices (Fig. S1). Subsequent phylogenetic tree using the neighbor-joining method revealed that the 14–3–3 proteins could primarily cluster into  $\epsilon$  and non- $\epsilon$  subgroups (Figs. 1 and 2A). In each of the five species, the number of non- $\epsilon$  group members was greater than the number of  $\epsilon$  group members (Fig. S2). Notably, the homologous gene numbers in the other four species differed from those in *A. thaliana*, with *GRF3*

harboring highest number (6) of homologous genes. However, the homologous genes of *GRF11* were absent in *A. pumila*, while those of *GRF4*, *GRF5*, and *GRF13* were absent in *B. oleracea*.

### Gene structure and protein conserved motifs of 14–3–3 gene family members

Comparative gene structure analysis revealed that the non- $\epsilon$  group members had conserved gene structures, consisting of 4 exons and 3 introns, whereas the  $\epsilon$  group members had between 6 and 9 exons (Fig. 2B). Using the MEME (<http://meme-suite.org/tools/meme>) online tool, 10 conserved motifs were identified in the 108 14–3–3 proteins (Fig. 2C and D), with all members harboring motif3, 6, and 7, whereas motif8 and motif10 were only found in the non- $\epsilon$  and the  $\epsilon$  subgroups, respectively. Additionally, AIGRF11, CsGRF11-2, and ApGRF13-2 lacked motif1, motif2, and motif4, respectively (Fig. 2C). The similarities and differences in gene structure and

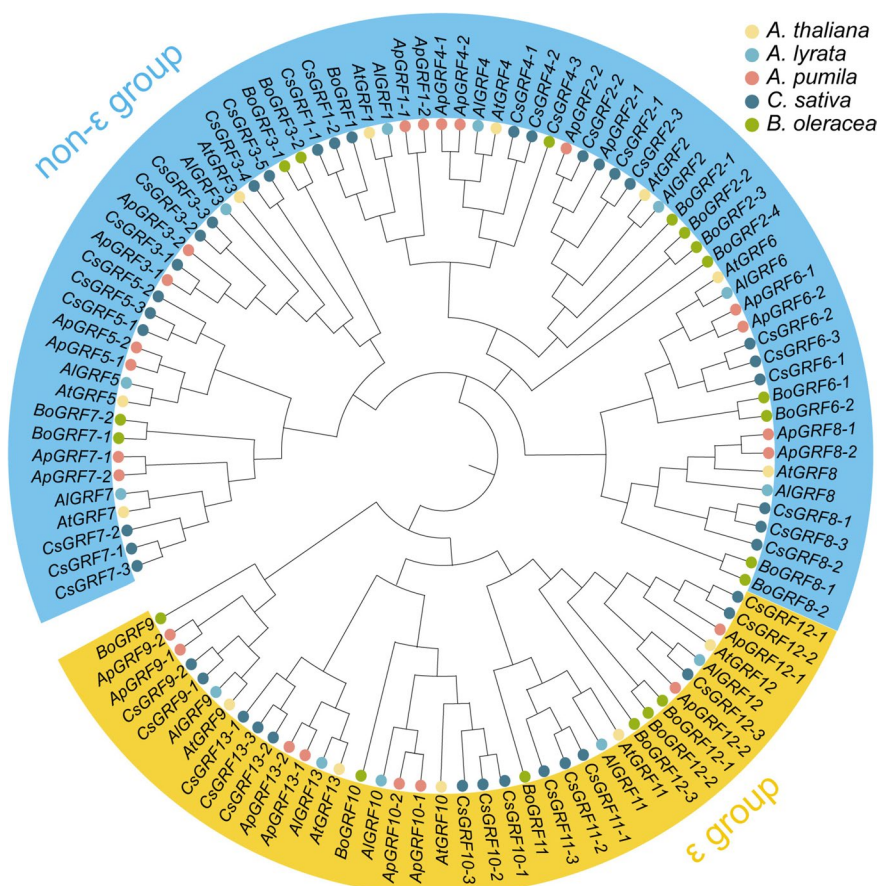


**Fig. 1** Phylogenetic tree of the 14–3–3 gene family members from five Brassicaceae species (circle tree). The neighbor-joining tree was constructed using 108 aligned 14–3–3 amino acid sequences from *A. thaliana* (13), *A. lyrata* (13), *A. pumila* (24), *C. sativa* (39), and *B. oleracea* (19) in MEGA11 [44], with bootstrap values calculated from 1000 replicates and parameters set to default values

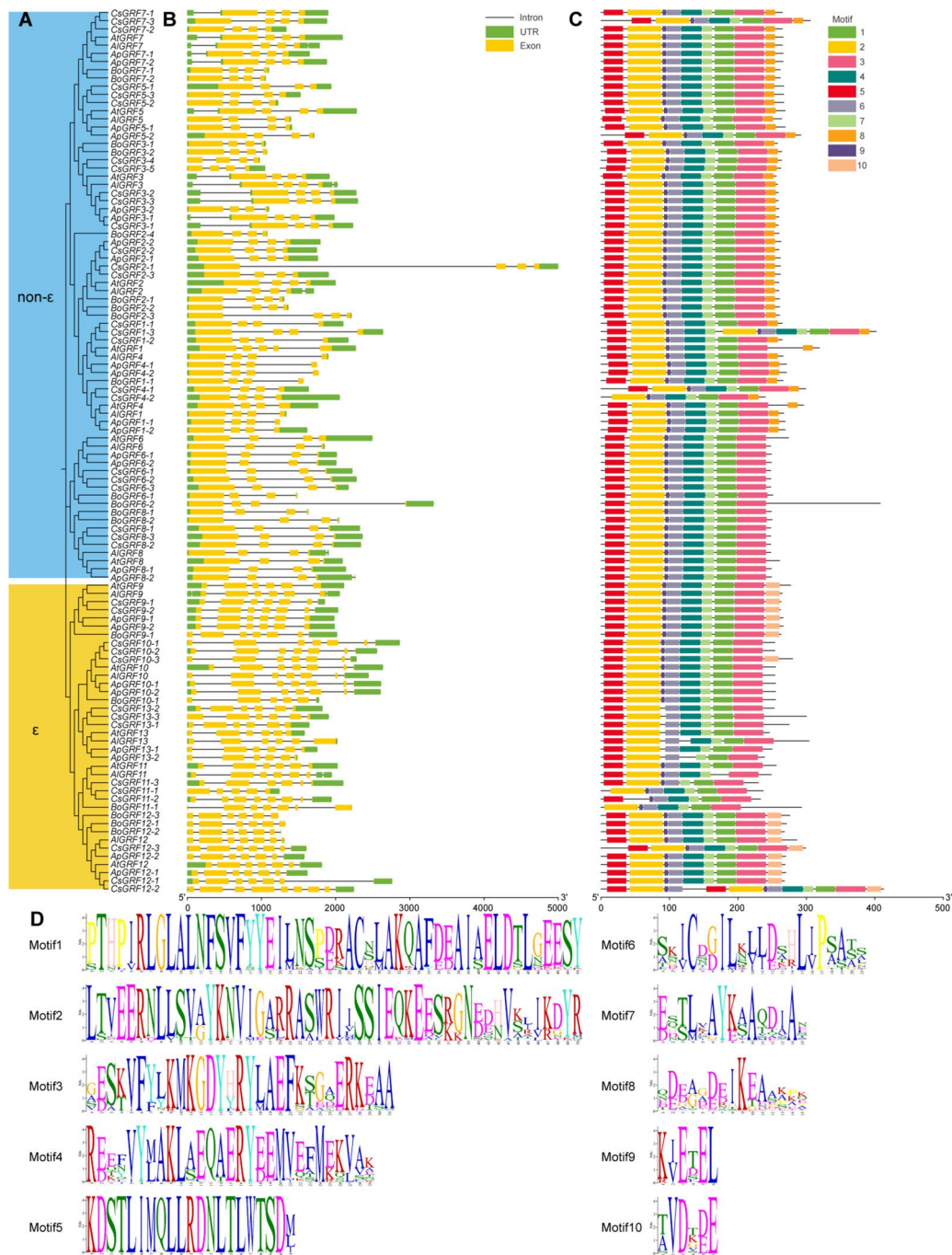


**Fig. 2** Phylogenetic relationships and structural characterization of 14-3-3 genes and conserved motifs in five Brassicaceae species. **A** Phylogenetic tree (branching tree) of 108 14-3-3 genes from five Brassicaceae species; **B** Intron-exon structures of the 14-3-3 genes in five Brassicaceae species; **C** and **D** Conserved motifs of 14-3-3 proteins in the five Brassicaceae species. The colors represent conserved motifs: 1-10

protein motif characteristics suggest that the 14-3-3 gene family has undergone both functional conservation and differentiation during its evolutionary history.

#### Inter-species collinearity of 14-3-3 gene members

To investigate the duplication and selective pressure of the 14-3-3 gene family members in Brassicaceae, MCS-canX [46] was used to analyze the collinearity relationship between *A. thaliana* and the other four species. The

results showed that collinear genes were only distributed on some chromosomes in each species (Fig. 3A). A total of 92 collinear gene pairs were found between *A. thaliana* and the other four Brassicaceae species (Table S5). Among them, each of the 13 *A. thaliana* 14–3–3 gene members shared collinear pairs with those of *A. lyrata*. An orthologous *AtGRF11* gene was deleted in *A. pumila*, *ApGRF1* had only one collinear gene pair with *A. thaliana*, while the remaining 11 *A. thaliana* 14–3–3 genes had two orthologous genes each in the *A. pumila* genome. For *C. sativa*, except for two homologs of *AtGRF4* and *AtGRF9*, the other 11 14–3–3 homologous genes were three times

their number in *A. thaliana*. *B. oleracea* had 4 *GRF2*, 3 *GRF12*, 2 *GRF3*, 2 *GRF6*, 2 *GRF7*, and 2 *GRF8*, and *GRF1*, *GRF9*, *GRF10*, and *GRF11* collinear gene pairs, but no collinear gene pairs for *GRF4*, *GRF5*, and *GRF13* (Fig. 3A). In summary, the 14–3–3 gene family members in the five studied Brassicaceae species have undergone both expansion and contraction during their evolutionary history, with expansion being more pronounced.

Analysis of the evolutionary selective pressure (*Ka/Ks*) on the orthologous 14–3–3 genes in the five Brassicaceae species revealed that 92 orthologous gene pairs had *Ka/Ks* values of < 1 (Table S5), indicating that the gene

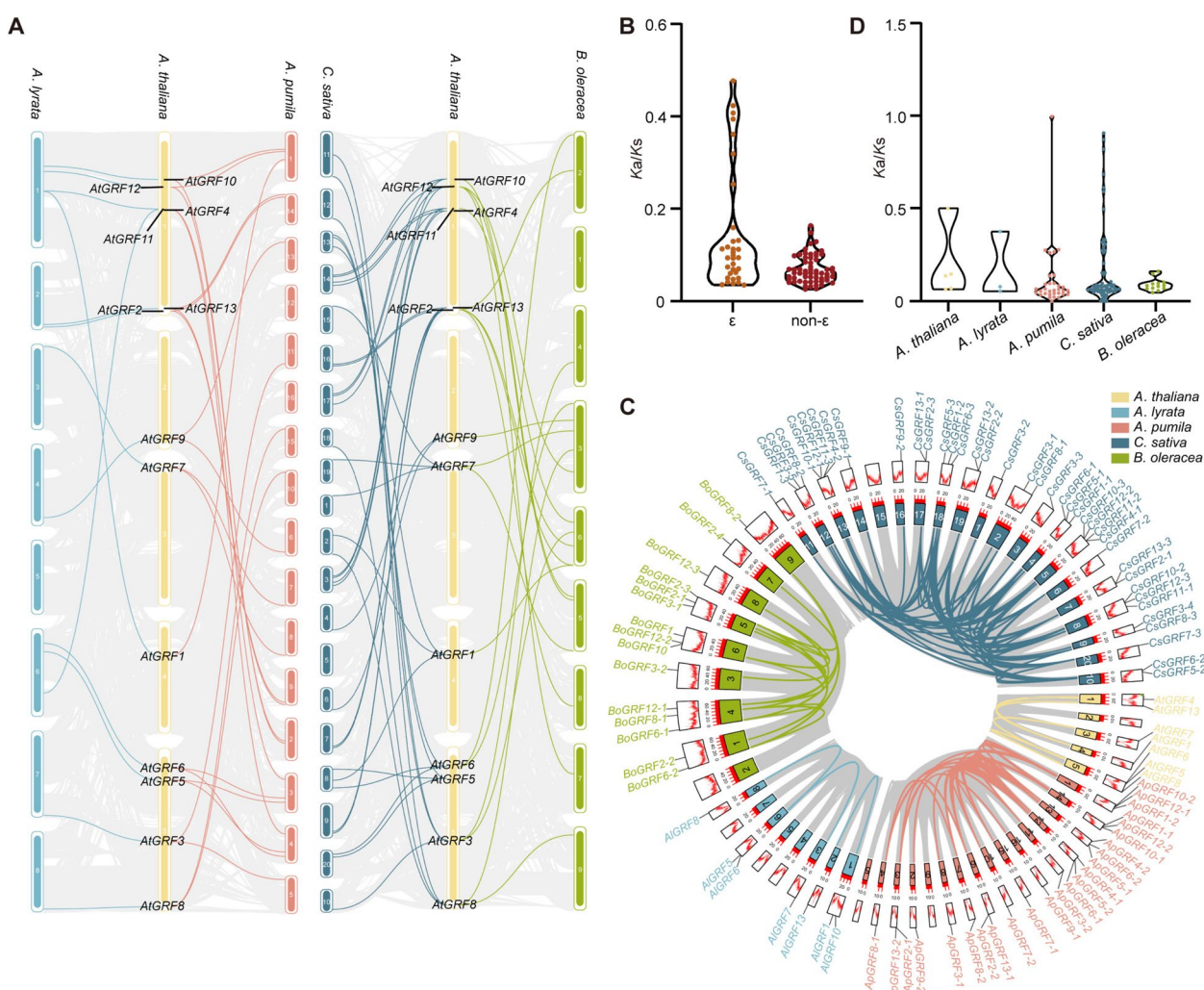


**Fig. 3** Inter-species and intra-species collinearity relationships and *Ka/Ks* values of 14–3–3 genes from five Brassicaceae species. **A** Analysis of inter-species collinearity relationships. Chromosomes are color-coded according to the corresponding species name. Gray lines represent all inter-species collinearity gene pairs, while colored lines represent collinear gene pairs between corresponding species and *A. thaliana*; **B** *Ka/Ks* values of  $\epsilon$  group and non- $\epsilon$  group inter-species 14–3–3 collinearity gene pairs; **C** Intra-species collinearity of 14–3–3 genes. Colored blocks represent chromosomes of the five species. The outer circle represents gene density on chromosomes. Gray lines represent all intra-species collinearity gene pairs, while colored lines represent collinear gene pairs within the corresponding species; **D** *Ka/Ks* values of intra-species 14–3–3 collinearity gene pairs

family has undergone strong purifying selection during evolution. Interestingly, average  $Ka/Ks$  value of the  $\epsilon$  group colinear gene pairs was larger than that of the non- $\epsilon$  group colinear gene pairs, suggesting that the  $\epsilon$  group genes have experienced relatively weaker purifying selection (Fig. 3B).

#### Intra-species collinearity of 14–3–3 gene members

Intra-species collinearity analysis of the 14–3–3 genes in *A. thaliana*, *A. lyrata*, *A. pumila*, *C. sativa*, and *B. oleracea* identified 127 colinear gene pairs (Fig. 3C and Table S6). Of these, the *C. sativa* genome had the largest number of colinear gene pairs, with 75 pairs; *A. lyrata* only had 3 pairs of paralogous homologs. *A. thaliana*, *A. pumila*, and *B. oleracea* had 6, 32, and 13 intra-species colinear gene pairs, respectively. Selective pressure analysis on the intra-species paralogous 14–3–3 gene pairs revealed that 122 pairs had  $Ka/Ks$  values of  $<1$ , indicating that most genes experienced purifying selection during evolution (Fig. 3D and Table S6). Only *ApGRF13-2/ApGRF13-1* colinear gene pair had  $Ka/Ks$  values slightly greater than 1, suggesting that it has almost not been subjected to natural selection pressure during evolution. Additionally, the  $Ka$  values for the *ApGRF6-2/ApGRF6-1*, *CsGRF4-1/CsGRF4-2*, *CsGRF6-1/CsGRF6-2*, and *CsGRF9-1/CsGRF9-2* gene pairs were zero, indicating high sequence similarity and the absence of non-synonymous substitutions.

#### Duplication history of the 14–3–3 gene family members in Brassicaceae species

Analysis of gene duplication revealed that the 108 14–3–3 genes could fall into four categories, with the majority occurring as whole-genome/segmental duplicates (WGD/S), while the remaining few occurring as dispersed, proximally, and tandemly duplicated genes (Table S7). WGD/S duplicated genes in *A. thaliana*, *A. lyrata*, *A. pumila*, *C. sativa*, and *B. oleracea* occurred in the frequency of 7 (53.3%), 6 (46.2%), 24 (100%), 14 (73.7%), and 39 (100%), respectively. Dispersed duplicated genes in *A. thaliana*, *A. lyrata*, and *B. oleracea* occurred in the frequency of 4 (30.8%), 7 (53.8%), and 5 (26.3%), respectively (Table S7).

#### Cis-elements screening in the 14–3–3 gene promoters

Screening of the 2.0 kb upstream promoter sequence regions of 108 14–3–3 genes identified 53 *cis*-acting element categories, including those responsive to light, growth and development, hormones, and abiotic stress. Light-responsive elements, such as Box 4, G-box, GT1-motif, and TCT-motif were predominantly detected in most of the 14–3–3 genes (Table S8). Similarly, *cis*-elements associated with growth and development-related,

such as GCN4-motif and O<sub>2</sub>-site as well as hormone-responsive elements, such as ABRE, TGA-element, CGTCA-motif, and TCA-element were predominantly detected in 14–3–3 genes. Other *cis*-elements involved in abiotic stress responses, such as GC-motif, TC-rich repeats, ARE, MBS, LTR, and WUN-motif were also detected. Among the identified *cis*-elements, light-responsive elements were the most abundant across the five Brassicaceae species, while growth and development-related elements were the least abundant (Fig. S3). Moreover, the enrichment patterns of *cis*-elements in the 14–3–3 gene promoters varied among different species (Fig. S4), which reflected the diverse functions of this gene family in Brassicaceae.

#### Tissue-specific expression patterns of 14–3–3 genes in *A. pumila*

To explore the potential roles of *A. pumila* 14–3–3 genes in plant growth and development, RNA-seq data from seven tissues, including cotyledons, hypocotyls, stems, rosette leaves, roots, flowers, and siliques were used to generate tissue expression heatmaps for 24 *A. pumila* 14–3–3 genes (Fig. 4A). The results showed that the expression patterns of these genes could be clustered into three main groups, designated C1, C2, and C3. Most members of the C1 group were highly expressed in the cotyledons and hypocotyls, but with lower expression in other tissues. However, one of the C1 members, *ApGRF2-2*, was specifically expressed in the hypocotyls and nearly undetectable in other tissues (Fig. 4A). Most of the C2 class genes showed high expression in siliques, with some also being highly expressed in flowers, while *ApGRF7-1* was highly expressed in the stems (Fig. 4A). The C3 class members, including *ApGRF1-1/2*, *ApGRF10-1/2*, and *ApGRF12-1/2*, showed tissue-specific expression in stems, roots, and flowers, respectively, but with diminished expression in other tissues (Fig. 4A). Additionally, qRT-PCR analysis confirmed that *ApGRF3-1/2* were predominantly expressed in siliques (Fig. 4B). Notably, *ApGRF4-1/2* and *ApGRF6-1/2* were highly expressed in cotyledons and hypocotyls, but with diminished profiles in other tissues, while *ApGRF7-1/2* and *ApGRF9-1/2* showed expression patterns consistent with the heatmap results. The tissue-specific expression of different *Ap14-3-3* genes suggests that they may have functional specificity.

#### Expression patterns of *Ap14-3-3* genes under 250 mM NaCl stress

The expression profiles of 24 *Ap14-3-3* genes were analyzed in the transcriptome data of *A. pumila* under salt stress, and the profiles revealed three main patterns in response to salt stress, including C1, C2, and C3 (Fig. 5A).

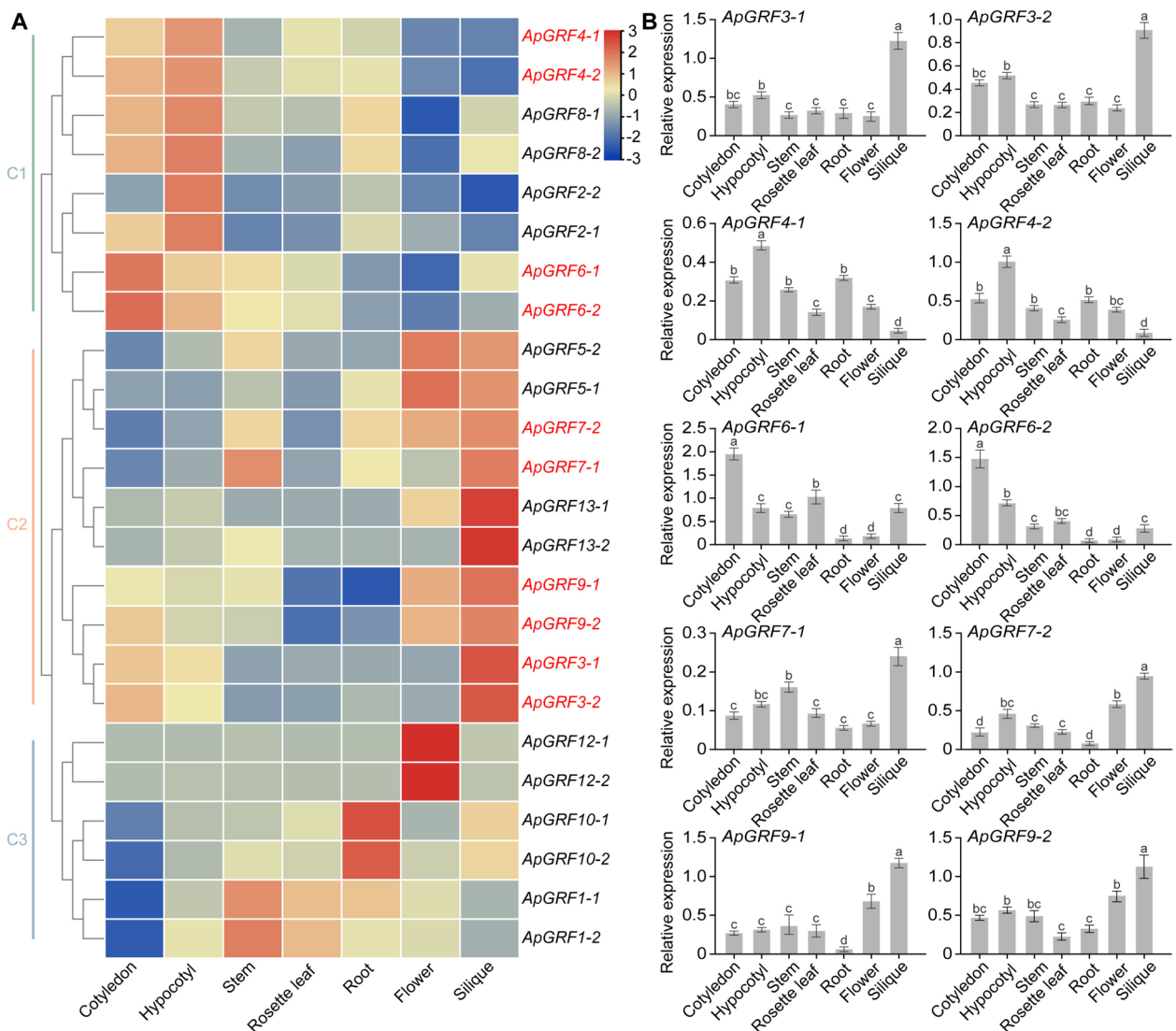


**Fig. 4** Tissue expression characteristics of *Ap14-3-3* genes. **A** RNA-seq based expression heatmap of 24 *Ap14-3-3* genes in cotyledons, hypocotyls, stems, rosette leaves, roots, flowers, and siliques; **B** qRT-PCR analysis of the gene names highlighted in red in **(A)**. Different lowercase letters represent statistically significant differences (Duncan multiple-range test,  $P < 0.05$ )

The C1 class showed a gradual increase in expression from 0 to 12 h under salt stress, followed by a gradual decrease from 12 to 48 h. In contrast, members of the C2 class were gradually downregulated after salt treatment. Most C3 class members showed gradual upregulated profiles after salt stress. However, *ApGRF1-2* and *ApGRF12-1* were significantly upregulated from 0 to 6 h before exhibiting gradual downregulation. *ApGRF2-1* and *ApGRF10-2* were upregulated from 0 to 24 h, then downregulated at 48 h (Fig. 5A). qRT-PCR results and RNA-seq data generally showed consistent expression profiles, however some genes exhibited inconsistent patterns (Fig. 5A and B). For instance, *ApGRF3-2*, *ApGRF4-1*, and *ApGRF7-1* showed induced

expression from 0 to 12 h, but with diminished profiles from 12 to 48 h under salt stress. The profiles of *ApGRF4-2*, *ApGRF6-1/2*, and *ApGRF9-1/2* were gradually downregulated after salt treatment, while *ApGRF3-1* and *ApGRF7-2* showed gradual upregulation in response to salt stress (Fig. 5B). The differential expression patterns of *Ap14-3-3* genes in response to prolonged salt stress suggested their crucial roles in salt stress response in *A. pumila*.

### Three-dimensional protein structure prediction of GRF6 protein and subcellular localization of ApGRF6-2 protein

The 3D structure predictions of nine proteins, including AtGRF6, AIGRF6, ApGRF6-1/2, BoGRF6-1/2, and

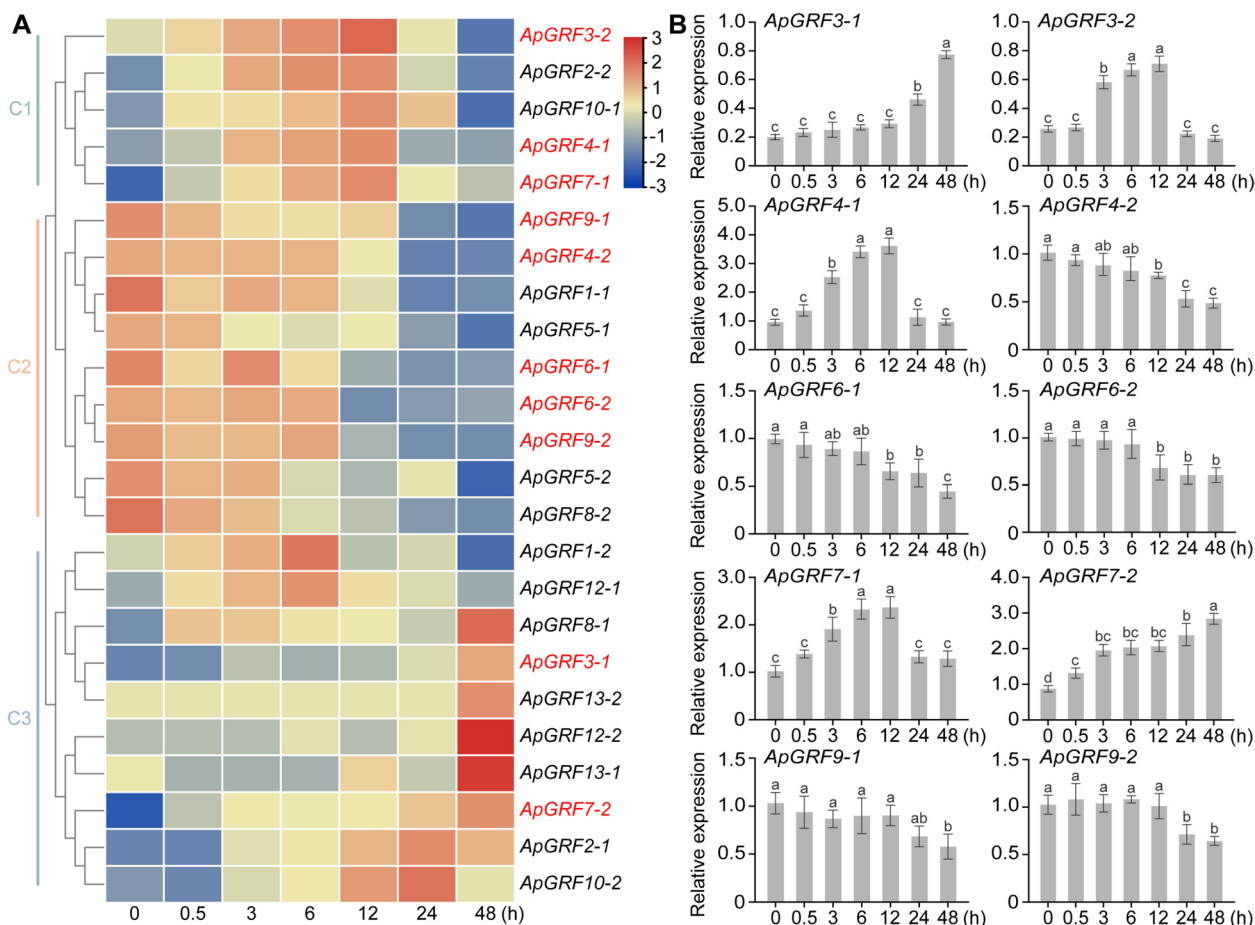


**Fig. 5** Expression characteristics of *Ap14-3-3* genes in response to sustained high salt stress. **A** RNA-seq based expression heatmap of 24 *Ap14-3-3* genes at seven different time points under sustained 250 mM NaCl salt stress; **B** qRT-PCR results of genes marked in red from (A). Different lowercase letters represent statistically significant differences (Duncan multiple-range test,  $P < 0.05$ )

CsGRF6-1/2/3 using AlphaFold 3 [52] indicated that all the proteins contained nine  $\alpha$ -helical structures, with  $\alpha 3$  and  $\alpha 4$  as the longest helices (Fig. 6A). These findings suggested that the GRF6 protein structure is highly conserved across different species, indicating that their functions have also been conserved during evolution. Subcellular localization of ApGRF6-2 protein was analyzed by transforming *35S:ApGRF6-2-GFP* vector in *A. thaliana* protoplasts followed by fluorescence observation, which revealed both cytoplasm and nucleus localization of ApGRF6-2 protein (Fig. 6B).

**Ectopic overexpression of *ApGRF6-2* gene promotes flowering in *A. thaliana***

Seven independent *35S:ApGRF6-2* transgenic wild-type *A. thaliana* (Col-0) lines with similar phenotypes were generated in this study. Notably, transgenic lines flowered earlier than the wild-type Col-0 plants (Fig. 7A, B, and Table S9). Under LD conditions, the homozygous

$T_3$  generation *35S:ApGRF6-2* transgenic plants flowered 6–8 d earlier than the wild-type Col-0, and with significantly reduced of rosette leaves at flowering (Fig. 7C, D, and Table S9). However, compared with Col-0, the *35S:ApGRF6-2* transgenic plants did not show obvious differences in leaf size, plant height, and seed yield. qRT-PCR confirmed that the expression of the *ApGRF6-2* gene in the transgenic *A. thaliana* plants was significantly higher than in the wild-type plants (Fig. 7E). Additionally, the endogenous flowering genes, *FRUITFULL* (*AtFUL*), *APETALA1* (*AtAPI*), and *SUPPRESSOR OF OVEREXPRESSION OF CONSTANS 1* (*AtSOC1*) in the *35S:ApGRF6-2 A. thaliana* plants showed varying upregulated degrees under LD conditions (Fig. 7F-H).

**Discussion**

The 14–3–3 proteins are highly conserved homodimer or heterodimer eukaryotic proteins that can interact simultaneously with two different target proteins to form

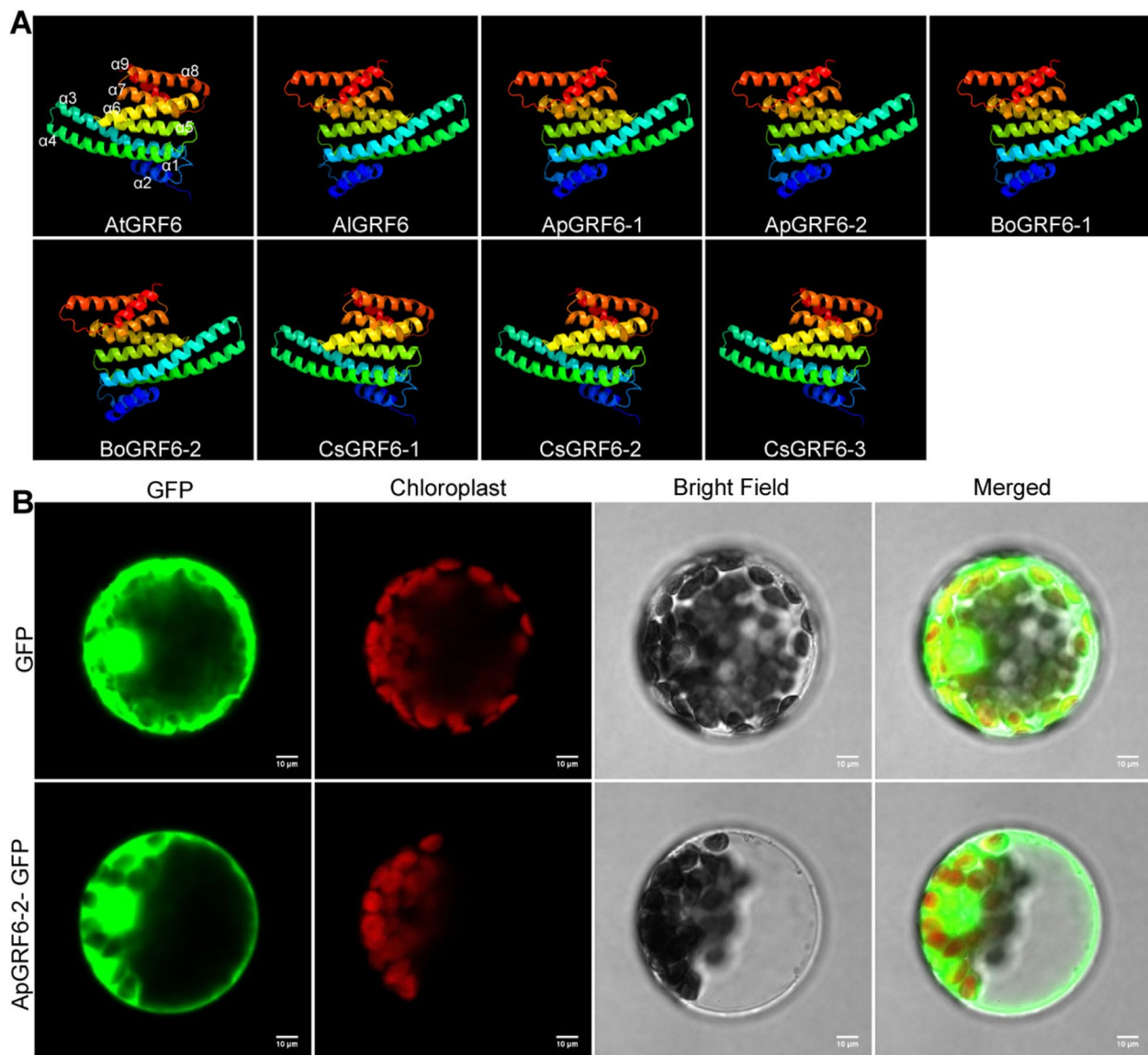


**Fig. 6** 3D structure prediction analysis of GRF6 protein and subcellular localization of ApGRF6-2 protein. **A** 3D structure prediction of AtGRF6, AIGRF6, ApGRF6-1/2, CsGRF6-1/2/3, and BoGRF6-1/2 proteins, with  $\alpha 1-9$  representing conserved motifs; **B** Subcellular localization of ApGRF6-2 protein in *A. thaliana* protoplasts

complexes with vital roles in various processes, such as plant growth, development, and stress responses [14, 57]. Despite their wide identification in numerous species [58, 59], systematic characterization and comparative evolutionary roles of 14-3-3 gene family in the Brassicaceae flowering process remain limited.

This study identified a total of 13, 24, 39, and 19 14-3-3 gene members from the genomes of *A. lyrata*, *A. pumila*, *C. sativa*, and *B. oleracea* (Table S1). Although *A. lyrata* has undergone a complete WGD event [30], the number of 14-3-3 gene family members in its genome remained similar to those of *A. thaliana*, suggesting that this gene

family remained relatively conserved during *A. lyrata* evolution [35]. However, the number of 14-3-3 gene family members increased varyingly in *A. pumila*, *C. sativa*, and *B. oleracea*, indicating that this gene family has undergone significant expansion during the evolutionary process of these species, which has likely contributed to their divergence and adaptation to changing environmental conditions [60]. However, further evaluating the underlying mechanisms of their functional divergence is still warranted.

Phylogenetic analysis showed that the 108 14-3-3 gene family members from the five species could be

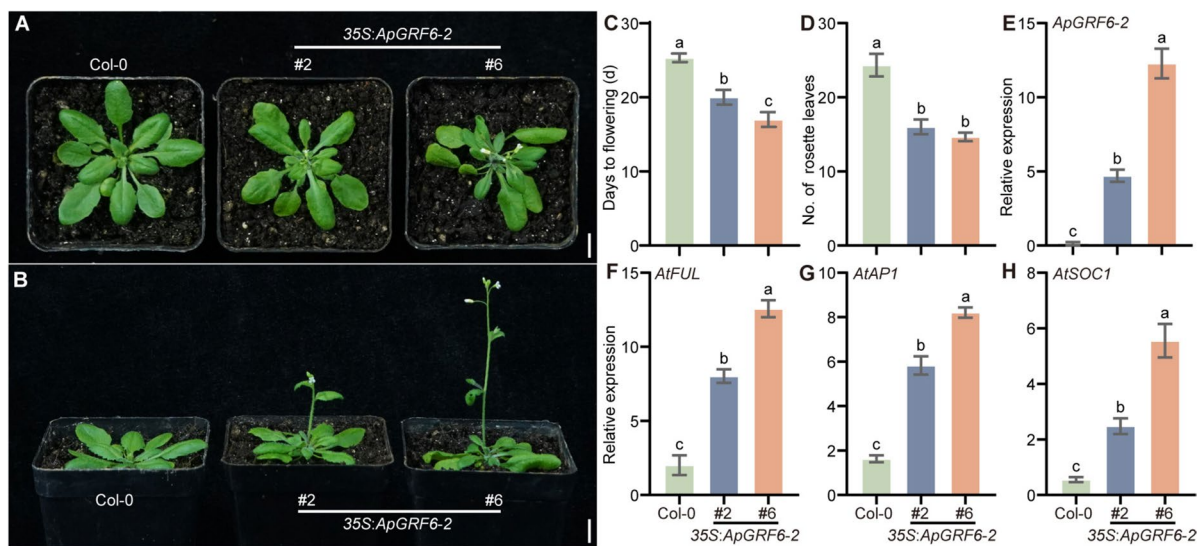


**Fig. 7** Phenotypic analysis of transgenic *A. thaliana* plants overexpressing *ApGRF6-2*. **A** and **B** Phenotypes of transgenic *A. thaliana* plants overexpressing *35S:ApGRF6-2* under LD conditions; **C** Comparative flowering-time phenotypes between the transgenic and wild-type *A. thaliana* plants; **D** Comparison of rosette leaf number at flowering between transgenic and wild-type *A. thaliana* plants; **E** Relative expression profiles of *ApGRF6-2* in the transgenic *A. thaliana* plants; **F–H** Relative expression levels of endogenous flowering genes in the transgenic and wild-type *A. thaliana* plants. The #2 and #6 represent two independent *35S:ApGRF6-2* transgenic lines. Scale bar: 1 cm. qRT-PCR was used to detect the expression levels of *ApGRF6-2*, *AtFUL*, *AtAP1*, and *AtSOC1* (**E–H**). Different lowercase letters indicate statistically significant differences (Duncan multiple-range test,  $P < 0.05$ )

categorized into  $\epsilon$  and non- $\epsilon$  groups, with fewer genes in the former than in the latter group (Figs. 1 and 2A). This finding is consistent with previous observation made in rice [61], *A. thaliana* [62], banana [63], and cotton [18]. Gene structure analysis revealed that the non- $\epsilon$  group members generally harbored fewer exons and introns compared to the  $\epsilon$  group members. Conserved motif analysis indicated that  $\epsilon$  and non- $\epsilon$  groups exhibited distinct motif structures, which was consistent with those observed in other species, suggesting their functional diversity (Fig. 2B–D) [18, 62]. Previous studies found that *AtGRF1-8*, the non- $\epsilon$  group *14-3-3* gene in *Arabidopsis*, mainly functions to regulate organ size and participate in response to low temperature stress [24, 64]. The  $\epsilon$  group members, *AtGRF9-13*, mainly respond to phosphorus stress [65]. In this study, we found that there were specific motifs between the members of the  $\epsilon$  and non- $\epsilon$  groups (Fig. 2C), suggesting that these motifs were highly likely the key factors in the functional differentiation of the  $\epsilon$  and non- $\epsilon$  genes. For example, motif8 is only present in non- $\epsilon$  group proteins, while motif10 is only present in  $\epsilon$  group proteins (Fig. 2C). We speculated that motif8 and motif10 may affect the functions of non- $\epsilon$  group and  $\epsilon$  group proteins by involving them in different signaling pathways or metabolic processes, ultimately leading to functional differences between the two groups.

Collinearity analysis which can predict genetic patterns and potential gene functions was used to identify

92 inter- and 127 intra-species collinear gene pairs in the five species studied. Moreover, few *14-3-3* genes in *A. pumila*, *C. sativa*, and *B. oleracea* formed more than one collinear gene pair, suggesting that these genes might harbor crucial evolutionary functions (Fig. 3A and C, Tables S5 and S6). *Ka/Ks* values of  $< 1$  was observed for all *14-3-3* orthologous genes between the five species (Table S5), indicating that purifying selection has potentially played a dominant role in maintaining the evolutionary functions of these genes, suggesting their critical basic physiological functions in these plants. When facing with sudden environmental changes, the  $\epsilon$  genes can quickly respond and adjust the physiological state of plants by changing their own structure and function [60], but changes in gene sequences may not necessarily lead to functional changes [66]. In this study, we found that compared to non- $\epsilon$  group genes, the purification selection of  $\epsilon$  group genes was relatively weaker (Fig. 3C). Therefore, during the evolution of Brassicaceae plants in response to rapidly changing environmental factors, the  $\epsilon$  group genes may have evolved more flexible regulatory mechanisms. Nearly all intra-species collinear gene pairs in the five species had *Ka/Ks* values of  $< 1$ , except for the *ApGRF13-2/ApGRF13-1* collinear gene pair, which had a value slightly greater than 1 (Table S6). The result suggested that this collinear gene pair might be under adaptive evolutionary process, potentially to generate new phenotypes that could be beneficial for plant survival

and reproduction. The *cis*-elements identified in the promoters of the 108 *14-3-3* genes showed association with various responses (Fig. S3 and Table S8), indicating their functional diversity. This study found that light-responsive elements accounted for the highest proportion in the prediction of promoter *cis*-acting elements of 108 *14-3-3* genes (Fig. S3), suggesting that *14-3-3* proteins may be involved in regulating the adaptive responses of plants to different light qualities and intensities, thereby affecting important physiological processes in plants such as photosynthesis, growth direction, and flowering time. Previous studies have found that the At14-3-3 proteins in *Arabidopsis* regulates root growth and chloroplast development as a component of the light-sensing system [67]. In the light signal transduction pathway, *14-3-3* proteins are highly likely to interact with photoreceptors or downstream signaling molecules, achieving fine-tuning of light response by regulating the expression of related genes [68].

Tissue expression analysis showed differential expression of *Ap14-3-3* genes in all the tissues studied, suggesting tissue-specific expression patterns (Fig. 4A), which is consistent with the profiles of *14-3-3* genes of other plants. For example, the *A. thaliana* *AtGRF1* gene showed expression in roots, flowers, and fruits, but not in leaves or cotyledons [2]. Similarly, the *V. vinifera* *VviGRF12* gene only exhibited high expression profiles in certain floral organs [17]. The observed tissue-specific expression of *Ap14-3-3* genes suggests that functional differentiation might have occurred during evolution. Previous functional studies of *14-3-3* genes under salt stress have revealed that the gene family can either enhance or negatively regulate plant salt tolerance. For instance, the rice *OsGRF6* could enhance salt tolerance by reducing H<sub>2</sub>O<sub>2</sub> accumulation and increasing reactive oxygen species (ROS) scavenging enzyme activity [69]. Conversely, *Malus pumila* MdGRF6-overexpressing plants exhibited enhanced salt stress sensitivity compared to wild-type plants [70]. In this study, the expression of genes, such as *ApGRF3-1* and *ApGRF7-2* were continuously upregulated after salt stress treatment, while others, such as *ApGRF4-2* and *ApGRF6-1* showed continuous down-regulation profiles (Fig. 5A). These results suggest that *Ap14-3-3* genes could both positively and/or negatively regulate salt stress response in *A. pumila*. Overall, results demonstrated that different members of the *14-3-3* gene family had distinct roles in plant salt stress responses, suggesting their functional diversity for improved plant adaptation to the environment.

The FAC is composed of the florigen FT, *14-3-3*, and FD proteins, and is responsible for promoting flowering by activating downstream target genes [21, 71, 72]. The 3D structure of GRF6 homologous proteins from five

Brassicaceae species showed a high degree of similarity, while subcellular localization confirmed that ApGRF6-2 protein is both localized in the cytoplasm and the nucleus (Fig. 6A and B), which was consistent with the subcellular localization of the cotton GhFT1 protein [54]. Moreover, *35S:ApGRF6-2* transgenic plants in this study had enhanced expression levels of the endogenous flowering genes *AtFUL*, *AtAPI*, and *AtSOC1*, resulting in reduced number of rosette leaves and activated early flowering (Fig. 7A-H and Table S9). *AtGRF6* was relatively highly expressed in SAM and flower buds of *Arabidopsis*, but its expression level is very low in mature flowers. *AtGRF6* may be involved in the process of flowering regulation [73]. These data suggest that *14-3-3*, as an important component of the FAC in Brassicaceae, could regulate flowering time in plants. However, the molecular mechanism by which *ApGRF6-2* regulates flowering in *A. pumila* requires further investigation. Moreover, we should explore the specific components of the *A. pumila* FAC and the molecular mechanisms underlying its adaptation to rapid flowering in desert environments. In addition, future studies will focus on the following directions: i) molecular mechanism of *ApGRF6-2* in regulating flowering through the FAC, combined with gene editing techniques to verify the functional differences of the  $\epsilon$ /non- $\epsilon$  subfamilies and the roles of motif8/10; ii) evolutionary driving forces and tissue-specific expression networks of *14-3-3* genes in Brassicaceae; iii) potential application of the *14-3-3* genes in Brassicaceae plants for crop stress resistance and flowering time regulation, as well as its interaction with other environmental factors.

## Conclusion

In summary, this study identified 13, 24, 39, and 19 *14-3-3* genes from the whole genomes of *A. lyrata*, *A. pumila*, *C. sativa*, and *B. oleracea*, respectively. The number of *14-3-3* genes were not directly proportional to the sizes of the plant genomes. Overall, the 108 *14-3-3* proteins from the five species could be classified into  $\epsilon$  and non- $\epsilon$  group, based on phylogenetic analysis. Structural features, inter-species and intra-species collinearity, gene duplication types, and *cis*-regulatory elements both revealed the conservation and diversity of *14-3-3* gene functions in Brassicaceae species. The *Ap14-3-3* genes exhibited tissue-specific expression and showed functional differentiation by positively and/or negatively regulating salt stress responses. Overexpression of *ApGRF6-2* could promote flowering by enhancing the expression of floral meristem identity genes. This study provides important insights into the functional mechanisms of the *14-3-3* gene family in growth, development, stress adaptation, and flowering regulation of Brassicaceae species. The results could lay crucial foundation for further

exploration of the molecular mechanisms underlying rapid flowering transformation of the desert *A. pumila* plant.

#### Abbreviations

<i>A. thaliana</i>	<i>Arabidopsis thaliana</i>
<i>A. lyrata</i>	<i>Arabidopsis lyrata</i>
<i>A. pumila</i>	<i>Arabidopsis pumila</i>
<i>C. sativa</i>	<i>Camelina sativa</i>
<i>B. oleracea</i>	<i>Brassica oleracea</i>
MW	Molecular weight
pI	Isoelectric points
<i>At14-3-3</i>	14-3-3 Genes of <i>Arabidopsis thaliana</i>
<i>Al14-3-3</i>	14-3-3 Genes of <i>Arabidopsis lyrata</i>
<i>Ap14-3-3</i>	14-3-3 Genes of <i>Arabidopsis pumila</i>
<i>Cs14-3-3</i>	14-3-3 Genes of <i>Camelina sativa</i>
<i>Bo14-3-3</i>	14-3-3 Genes of <i>Brassica oleracea</i>

#### Supplementary Information

The online version contains supplementary material available at <https://doi.org/10.1186/s12864-025-11513-0>.

Supplementary Material 1.  
Supplementary Material 2.

#### Authors' contributions

XH conceived and designed the experiments. JZ and SL performed most of the experiments. HR, E O A, and MZ analyzed the data. JZ and DX draft the manuscript. XH supervised and complemented the writing. All authors have reviewed the manuscript.

#### Funding

This work was supported by the National Natural Science Foundation of China (32270385), the Scientific and Technological Innovation Team of Anhui Science and Technology University (2023KJCXTD001), the Excellent Scientific Research and Innovation Team of the Education Department of Anhui Province (2022AH010087), the Talent Introduction Start-up Fund Project of Anhui Science and Technology University (NXJY202001), the Key Discipline Construction Fund for Crop Science of Anhui Science and Technology University (XK-XJGF001). National Natural Science Foundation of China,32270385,Scientific and Technological Innovation Team of Anhui Science and Technology University,2023KJCXTD001,Excellent Scientific Research and Innovation Team of the Education Department of Anhui Province,2022AH010087,Talent Introduction Start-up Fund Project of Anhui Science and Technology University,NXJY202001,Key Discipline Construction Fund for Crop Science of Anhui Science and Technology University,XK-XJGF001

#### Data availability

The genome data for *A. lyrata*, *C. sativa*, and *B. oleracea* were downloaded from the Ensembl Plants genome database (<https://plants.ensembl.org>), while the *A. thaliana* genome data (TAIR10.1) was obtained from the Arabidopsis Information Resource website (TAIR, <https://www.arabidopsis.org>). Accession numbers for the RNA-seq data of leaves exposed to salt stress at 0.5, 3, 6, 12, 24 and 48 h are SRR6320595, SRR6320596, SRR6320597, SRR6320598, SRR6320599, SRR6320600 and SRR6320601 under BioProject PRJNA417986 at the SRA database (<https://www.ncbi.nlm.nih.gov/sra>). Accession numbers for the RNA-seq data of cotyledons, hypocotyls, stems, rosette leaves, roots, flowers, and siliques are SRR14470721, SRR14470718, SRR14470723, SRR14470714, SRR14470717, SRR14470719 and SRR14470724 under BioProject PRJNA728218 at the SRA database (<https://www.ncbi.nlm.nih.gov/sra>).

#### Declarations

##### Ethics approval and consent to participate

Not applicable.

##### Consent for publication

Not applicable.

##### Competing interests

The authors declare no competing interests.

Received: 6 January 2025 Accepted: 20 March 2025

Published online: 29 March 2025

#### References

- Aitken A, Collinge DB, van Heusden BP, Isobe T, Roseboom PH, Rosenfeld G, Soll J. 14-3-3 proteins: a highly conserved, widespread family of eukaryotic proteins. *Trends Biochem Sci.* 1992;17(12):498–501.
- Daugherty CJ, Rooney MF, Miller PW, Ferl RJ. Molecular organization and tissue-specific expression of an Arabidopsis 14-3-3 gene. *Plant Cell.* 1996;8(8):1239–48.
- Wu K, Rooney MF, Ferl RJ. The Arabidopsis 14-3-3 multigene family. *Plant Physiol.* 1997;114(4):1421–31.
- Sehnke PC, DeLille JM, Ferl RJ. Consummating signal transduction: the role of 14-3-3 proteins in the completion of signal-induced transitions in protein activity. *Plant Cell.* 2002;14(Suppl):339–54.
- Gao J, van Kleeff PJ, Oecking C, Li KW, Erban A, Kopka J, Hincha DK, de Boer AH. Light modulated activity of root alkaline/neutral invertase involves the interaction with 14-3-3 proteins. *Plant J.* 2014;80(5):785–96.
- Chen YS, Ho TD, Liu L, Lee DH, Lee CH, Chen YR, Lin SY, Lu CA, Yu SM. Sugar starvation-regulated MYB2 and 14-3-3 protein interactions enhance plant growth, stress tolerance, and grain weight in rice. *Proc Natl Acad Sci U S A.* 2019;116(43):21925–35.
- Pallucca R, Visconti S, Camoni L, Cesareni G, Melino S, Torrerri P, Aducci P. Specificity of  $\epsilon$  and non- $\epsilon$  isoforms of *Arabidopsis* 14-3-3 proteins towards the H<sup>+</sup>-ATPase and other targets. *PLoS One.* 2014. <https://doi.org/10.1371/journal.pone.0090764>.
- Liu D, Bienkowska J, Petosa C, Collier RJ, Fu H, Liddington R. Crystal structure of the zeta isoform of the 14-3-3 protein. *Nature.* 1995;376(6536):191–4.
- Xiao B, Smerdon SJ, Jones DH, Dodson GG, Soneji Y, Aitken A, Gamblin SJ. Structure of a 14-3-3 protein and implications for coordination of multiple signalling pathways. *Nature.* 1995;376(6536):188–91.
- Yang X, Lee WH, Sobott F, Papagrigoriou E, Robinson CV, Grossmann JG, Sundström M, Doyle DA, Elkins JM. Structural basis for protein-protein interactions in the 14-3-3 protein family. *Proc Natl Acad Sci U S A.* 2006;103(46):17237–42.
- Muslin AJ, Tanner JW, Allen PM, Shaw AS. Interaction of 14-3-3 with signaling proteins is mediated by the recognition of phosphoserine. *Cell.* 1996;84(6):889–97.
- Yaffe MB, Rittinger K, Volinia S, Caron PR, Aitken A, Leffers H, Gamblin SJ, Smerdon SJ, Cantley LC. The structural basis for 14-3-3: phosphopeptide binding specificity. *Cell.* 1997;91(7):961–71.
- Ganguly S, Weller JL, Ho A, Chemineau P, Malpoux B, Klein DC. Melatonin synthesis: 14-3-3-dependent activation and inhibition of arylalkylamine N-acetyltransferase mediated by phosphoserine-205. *Proc Natl Acad Sci U S A.* 2005;102(4):1222–7.
- Sheikh AH, Zacharia I, Tabassum N, Hirt H, Ntoukakis V. 14-3-3 proteins as a major hub for plant immunity. *Trends Plant Sci.* 2024;29(11):1245–53.
- Coblitz B, Wu M, Shikano S, Li M. C-terminal binding: an expanded repertoire and function of 14-3-3 proteins. *FEBS Lett.* 2006;580(6):1531–5.
- Yao Y, Du Y, Jiang L, Liu JY. Molecular analysis and expression patterns of the 14-3-3 gene family from *Oryza sativa*. *J Biochem Mol Biol.* 2007;40(3):349–57.
- Cheng C, Wang Y, Chai F, Li S, Xin H, Liang Z. Genome-wide identification and characterization of the 14-3-3 family in *Vitis vinifera* L. during berry development and cold- and heat-stress response. *BMC Genomics.* 2018;19(1):579.
- Sang N, Liu H, Ma B, Huang X, Zhuo L, Sun Y. Roles of the 14-3-3 gene family in cotton flowering. *BMC Plant Biol.* 2021;21(1):162.
- He F, Duan S, Jian Y, Xu J, Hu J, Zhang Z, Lin T, Cheng F, Li G. Genome-wide identification and gene expression analysis of the 14-3-3 gene family in potato (*Solanum tuberosum* L.). *BMC Genomics.* 2022;23(1):811.

20. Zhang Y, He Y, Zhao H, Wang Y, Wu C, Zhao Y, Xue H, Zhu Q, Zhang J, Ou X. The 14-3-3 Protein BdGF14a Increases the Transcriptional Regulation Activity of *BdbZIP62* to Confer Drought and Salt Resistance in Tobacco. *Plants (Basel)*. 2024;13(2):245.
21. Taoka K, Ohki I, Tsuji H, Furuita K, Hayashi K, Yanase T, Yamaguchi M, Nakashima C, Purwestri YA, Tamaki S, Ogaki Y, Shimada C, Nakagawa A, Kojima C, Shimamoto K. 14-3-3 proteins act as intracellular receptors for rice Hd3a florigen. *Nature*. 2011;476(7360):332–5.
22. Li JJ, Lu TT, Mo WJ, Yu HX, Li KJ, Huang X, Fan ZY, He XH, Luo C. Functional characterization of *MIFTs* implicated in early flowering and stress resistances of mango. *Int J Biol Macromol*. 2024;280(Pt 1): 135669.
23. Pnueli L, Carmel-Goren L, Hareven D, Gutfinger T, Alvarez J, Ganal M, Zamir D, Lifschitz E. The SELF-PRUNING gene of tomato regulates vegetative to reproductive switching of sympodial meristems and is the ortholog of CEN and TFL1. *Development*. 1998;125(11):1979–89.
24. Liu Z, Jia Y, Ding Y, Shi Y, Li Z, Guo Y, Gong Z, Yang S. Plasma Membrane CRPK1-Mediated Phosphorylation of 14-3-3 Proteins Induces Their Nuclear Import to Fine-Tune CBF Signaling during Cold Response. *Mol Cell*. 2017;66(1):117–128.e5.
25. Luo J, Tang S, Peng X, Yan X, Zeng X, Li J, Li X, Wu G. Elucidation of cross-talk and specificity of early response mechanisms to salt and PEG-simulated drought stresses in *brassica napus* using comparative proteomic analysis. *PLoS One*. 2015;10(10): e0138974.
26. Liu L, Du X, Guo C, Li D. Resolving robust phylogenetic relationships of core Brassicaceae using genome skimming data. *J Syst Evol*. 2021;59(3):442–53.
27. De Smet R, Sabaghian E, Li Z, Saey Y, Van de Peer Y. Coordinated functional divergence of genes after genome duplication in *Arabidopsis thaliana*. *Plant Cell*. 2017;29(11):2786–800.
28. Bayat S, Lysak MA, Mandáková T. Genome structure and evolution in the cruciferous tribe Thlaspidaeae (Brassicaceae). *Plant J*. 2021;108(6):1768–85.
29. Das Laha S, Dutta S, Schäffner AR, Das M. Gene duplication and stress genomics in Brassicas: current understanding and future prospects. *J Plant Physiol*. 2020. <https://doi.org/10.1016/j.jplph.2020.153293>.
30. Cheng S, van den Bergh E, Zeng P, Zhong X, Xu J, Liu X, Hofberger J, de Bruijn S, Bhida AS, Kuelahoglu C, Bian C, Chen J, Fan G, Kaufmann K, Hall JC, Becker A, Bräutigam A, Weber AP, Shi C, Zheng Z, Li W, Lv M, Tao Y, Wang J, Zou H, Quan Z, Hibberd JM, Zhang G, Zhu XG, Xu X, Schranz ME. The *Tarenaya hassleriana* genome provides insight into reproductive trait and genome evolution of crucifers. *Plant Cell*. 2013;25(8):2813–30.
31. Wang X, Wang H, Wang J, Sun R, Wu J, Liu S, Bai Y, Mun JH, Bancroft I, Cheng F, Huang S, Li X, Hua W, Wang J, Wang X, Freeling M, Pires JC, Paterson AH, Chalhoub B, Wang B, Hayward A, Sharpe AG, Park BS, Weishaar B, Liu B, Li B, Liu B, Tong C, Song C, Duran C, Peng C, Geng C, Koh C, Lin C, Edwards D, Mu D, Shen D, Soumpourou E, Li F, Fraser F, Conant G, Lassalle G, King GJ, Bonnema G, Tang H, Wang H, Belcram H, Zhou H, Hirakawa H, Abe H, Guo H, Wang H, Jin H, Parkin IA, Batley J, Kim JS, Just J, Li J, Xu J, Deng J, Kim JA, Li J, Yu J, Meng J, Wang J, Min J, Poulain J, Wang J, Hatakeyama K, Wu K, Wang L, Fang L, Trick M, Links MG, Zhao M, Jin M, Ramchiary N, Drou N, Berkman PJ, Cai Q, Huang Q, Li R, Tabata S, Cheng S, Zhang S, Zhang S, Huang S, Sato S, Sun S, Kwon SJ, Choi SR, Lee TH, Fan W, Zhao X, Tan X, Xu X, Wang Y, Qiu Y, Yin Y, Li Y, Du Y, Liao Y, Lim Y, Narusaka Y, Wang Y, Wang Z, Li Z, Wang Z, Xiong Z, Zhang Z, Brassica rapa Genome Sequencing Project Consortium. The genome of the mesopolyploid crop species *Brassica rapa*. *Nat Genet*. 2011;43(10):1035–9.
32. Kagale S, Koh C, Nixon J, Bollina V, Clarke WE, Tuteja R, Spillane C, Robinson SJ, Links MG, Clarke C, Higgins EE, Huebert T, Sharpe AG, Parkin IA. The emerging biofuel crop *Camelina sativa* retains a highly undifferentiated hexaploid genome structure. *Nat Commun*. 2014;5:3706.
33. Arabidopsis Genome Initiative. Analysis of the genome sequence of the flowering plant *Arabidopsis thaliana*. *Nature*. 2000;200(408):796–815.
34. Bernal-Gallardo JJ, de Folter S. Plant genome information facilitates plant functional genomics. *Planta*. 2024;259(5):117.
35. Hu TT, Pattyn P, Bakker EG, Cao J, Cheng JF, Clark RM, Fahlgren N, Fawcett JA, Grimwood J, Gundlach H, Haberer G, Hollister JD, Ossowski S, Ottillar RP, Salamov AA, Schneeberger K, Spannagl M, Wang X, Yang L, Nasrallah ME, Bergelson J, Carrington JC, Gaut BS, Schmutz J, Mayer KF, Van de Peer Y, Grigoriev IV, Nordborg M, Weigel D, Guo YL. The *Arabidopsis lyrata* genome sequence and the basis of rapid genome size change. *Nat Genet*. 2011;43(5):476–81.
36. Liu S, Liu Y, Yang X, Tong C, Edwards D, Parkin IA, Zhao M, Ma J, Yu J, Huang S, Wang X, Wang J, Lu K, Fang Z, Bancroft I, Yang TJ, Hu Q, Wang X, Yue Z, Li H, Yang L, Wu J, Zhou Q, Wang W, King GJ, Pires JC, Lu C, Wu Z, Sampath P, Wang Z, Guo H, Pan S, Yang L, Min J, Zhang D, Jin D, Li W, Belcram H, Tu J, Guan M, Qi C, Du D, Li J, Jiang L, Batley J, Sharpe AG, Park BS, Ruperao P, Cheng F, Waminal NE, Huang Y, Dong C, Wang L, Li J, Hu Z, Zhuang M, Huang Y, Huang J, Shi J, Mei D, Liu J, Lee TH, Wang J, Jin H, Li Z, Li X, Zhang J, Xiao L, Zhou Y, Liu Z, Liu X, Qin R, Tang X, Liu W, Wang Y, Zhang Y, Lee J, Kim HH, Denoed F, Xu X, Liang X, Hua W, Wang X, Wang J, Chalhoub B, Paterson AH. The Brassica oleracea genome reveals the asymmetrical evolution of polyploid genomes. *Nat Commun*. 2014;5:3930.
37. Guo N, Wang S, Gao L, Liu Y, Wang X, Lai E, Duan M, Wang G, Li J, Yang M, Zong M, Han S, Pei Y, Borm T, Sun H, Miao L, Liu D, Yu F, Zhang W, Ji H, Zhu C, Xu Y, Bonnema G, Li J, Fei Z, Liu F. Genome sequencing sheds light on the contribution of structural variants to Brassica oleracea diversification. *BMC Biol*. 2021;19(1):93.
38. Tu W, Li Y, Liu W, Wu L, Xie X, Zhang Y, Wilhelm C, Yang C. Spring Ephemerals Adapt to Extremely High Light Conditions via an Unusual Stabilization of Photosystem II. *Front Plant Sci*. 2016;6:1189.
39. Yang L, Jin Y, Huang W, Sun Q, Liu F, Huang X. Full-length transcriptome sequences of ephemeral plant *Arabidopsis pumila* provides insight into gene expression dynamics during continuous salt stress. *BMC Genomics*. 2018;19(1):71.
40. Jin Y, Guo L, Liu D, Li Y, Ai H, Huang X. Techniques for the regeneration and genetic transformation of *Arabidopsis pumila*: an ephemeral plant suitable for investigating the mechanisms for adaptation to desert environments. *Plant Cell Tiss Org*. 2022;150(1):237–46.
41. Li YG, Jin YH, Guo L, Ai H, Li RN, Huang XZ. Genome-wide identification and expression analysis of the *PEBP* genes in *Arabidopsis pumila*. *Yi Chuan*. 2022;44:80–94.
42. Jin S, Zhang X, Nie Y, Guo X, Liang S, Zhu H. Identification of a novel elite genotype for in vitro culture and genetic transformation of cotton. *Biol Plant*. 2006;50:519–24.
43. Thompson JD, Gibson TJ, Higgins DG. Multiple sequence alignment using ClustalW and ClustalX. *Curr Protoc Bioinformatics*. 2002. <https://doi.org/10.1002/0471250953.bi0203s00>.
44. Tamura K, Stecher G, Kumar S. MEGA11: molecular evolutionary genetics analysis version 11. *Mol Biol Evol*. 2021;38(7):3022–7.
45. Chen C, Wu Y, Li J, Wang X, Zeng Z, Xu J, Liu Y, Feng J, Chen H, He Y, Xia R. TBtools-II: A “one for all, all for one” bioinformatics platform for biological big-data mining. *Mol Plant*. 2023;16(11):1733–42.
46. Wang Y, Tang H, Debarry JD, Tan X, Li J, Wang X, Lee TH, Jin H, Marler B, Guo H, Kissinger JC, Paterson AH. MCScanX: a toolkit for detection and evolutionary analysis of gene synteny and collinearity. *Nucleic Acids Res*. 2012. <https://doi.org/10.1093/nar/gkr1293>.
47. Rozas J, Ferrer-Mata A, Sánchez-DelBarrio JC, Guirao-Rico S, Librado P, Ramos-Onsins SE, Sánchez-Gracia A. DnaSP 6: DNA sequence polymorphism analysis of large data sets. *Mol Biol Evol*. 2017;34(12):3299–302.
48. Yadav CB, Bonthala VS, Muthamilaran M, Pandey G, Khan Y, Prasad M. Genome-wide development of transposable elements-based markers in foxtail millet and construction of an integrated database. *DNA Res*. 2015;22(1):79–90.
49. Trapnell C, Williams BA, Pertea G, Mortazavi A, Kwan G, van Baren MJ, Salzberg SL, Wold BJ, Pachter L. Transcript assembly and quantification by RNA-Seq reveals unannotated transcripts and isoform switching during cell differentiation. *Nat Biotechnol*. 2010;28(5):511–5.
50. Jin Y, Liu F, Huang W, Sun Q, Huang X. Identification of reliable reference genes for qRT-PCR in the ephemeral plant *Arabidopsis pumila* based on full-length transcriptome data. *Sci Rep*. 2019;9(1):8408.
51. Livak KJ, Schmittgen TD. Analysis of relative gene expression data using real-time quantitative PCR and the 2<sup>-ΔΔC<sub>T</sub></sup> method. *Meth-ods*. 2001;25(4):402–8.
52. Abramson J, Adler J, Dunger J, Evans R, Green T, Pritzel A, Ronneberger O, Willmore L, Ballard AJ, Bambrick J, Bodenstein SW, Evans DA, Hung CC, O'Neill M, Reiman D, Tunyasuvunakool K, Wu Z, Žemgulytė A, Arvaniti E, Beattie C, Bertolli O, Bridgland A, Cherepanov A, Congreve M, Cowen-Rivers AI, Cowie A, Figurnov M, Fuchs FB, Gladman H, Jain R, Khan YA, Low CMR, Perlin K, Potapenko A, Savy P, Singh S, Stecula A, Thillaisundaram A, Tong C, Yakneen S, Zhong ED, Zielinski M, Židek A, Bapst V, Kohli P, Jaderberg M, Hassabis D, Jumper JM. Accurate structure

- prediction of biomolecular interactions with AlphaFold 3. *Nature*. 2024;630(8016):493–500.
53. Meng EC, Goddard TD, Pettersen EF, Couch GS, Pearson ZJ, Morris JH, Ferrin TE. UCSF ChimeraX: Tools for structure building and analysis. *Protein Sci*. 2023. <https://doi.org/10.1002/pro.4792>.
  54. Guo D, Li C, Dong R, Li X, Xiao X, Huang X. Molecular cloning and functional analysis of the *FLOWERING LOCUS T (FT)* homolog *GhFT1* from *Gossypium hirsutum*. *J Integr Plant Biol*. 2015;57(6):522–33.
  55. Liu H, Huang X, Ma B, Zhang T, Sang N, Zhuo L, Zhu J. Components and functional diversification of florigen activation complexes in cotton. *Plant Cell Physiol*. 2021;62(10):1542–55.
  56. Clough SJ, Bent AF. Floral dip: a simplified method for *Agrobacterium*-mediated transformation of *Arabidopsis thaliana*. *Plant J*. 1998;16(6):735–43.
  57. Paul AL, Denison FC, Schultz ER, Zupanska AK, Ferl RJ. 14-3-3 phosphoprotein interaction networks - does isoform diversity present functional interaction specification? *Front Plant Sci*. 2012;3:190.
  58. Yang L, You J, Wang Y, Li J, Quan W, Yin M, Wang Q, Chan Z. Systematic analysis of the G-box Factor 14-3-3 gene family and functional characterization of GF14a in *Brachypodium distachyon*. *Plant Physiol Biochem*. 2017;117:1–11.
  59. Lu Y, Meng Y, Zeng J, Luo Y, Feng Z, Bian L, Gao S. Coordination between GROWTH-REGULATING FACTOR1 and GRF-INTERACTING FACTOR1 plays a key role in regulating leaf growth in rice. *BMC Plant Biol*. 2020;20(1):200.
  60. Ren J, Zhang P, Dai Y, Liu X, Lu S, Guo L, Gou H, Mao J. Evolution of the 14-3-3 gene family in monocotyledons and dicotyledons and validation of *MdGRF13* function in transgenic *Arabidopsis thaliana*. *Plant Cell Rep*. 2023;42(8):1345–64.
  61. Chen F, Li Q, Sun L, He Z. The rice 14-3-3 gene family and its involvement in responses to biotic and abiotic stress. *DNA Res*. 2006;13(2):53–63.
  62. Chevalier D, Morris ER, Walker JC. 14-3-3 and FHA domains mediate phosphoprotein interactions. *Annu Rev Plant Biol*. 2009;60:67–91.
  63. Li M, Ren L, Xu B, Yang X, Xia Q, He P, Xiao S, Guo A, Hu W, Jin Z. Genome-Wide Identification, Phylogeny, and Expression Analyses of the 14-3-3 Family Reveal Their Involvement in the Development, Ripening, and Abiotic Stress Response in Banana. *Front Plant Sci*. 2016;7:1442.
  64. Kim JH, Choi D, Kende H. The AtGRF family of putative transcription factors is involved in leaf and cotyledon growth in *Arabidopsis*. *Plant J*. 2003;36(1):94–104.
  65. Zhang L, Li G, Li Y, Min J, Kronzucker HJ, Shi W. Tomato plants ectopically expressing *Arabidopsis GRF9* show enhanced resistance to phosphate deficiency and improved fruit production in the field. *J Plant Physiol*. 2018;226:31–9.
  66. Shen X, Song S, Li C, Zhang J. Synonymous mutations in representative yeast genes are mostly strongly non-neutral. *Nature*. 2022;606(7915):725–31.
  67. Mayfield JD, Paul AL, Ferl RJ. The 14-3-3 proteins of *Arabidopsis* regulate root growth and chloroplast development as components of the photosensory system. *J Exp Bot*. 2012;63(8):3061–70.
  68. Song P, Yang Z, Guo C, Han R, Wang H, Dong J, Kang D, Guo Y, Yang S, Li J. 14-3-3 proteins regulate photomorphogenesis by facilitating light-induced degradation of PIF3. *New Phytol*. 2023;237(1):140–59.
  69. Yuan H, Cheng M, Wang R, Wang Z, Fan F, Wang W, Si F, Gao F, Li S. miR396b/GRF6 module contributes to salt tolerance in rice. *Plant Biotechnol J*. 2024;22(8):2079–92.
  70. Zhu Y, Kuang W, Leng J, Wang X, Qiu L, Kong X, Wang Y, Zhao Q. The apple 14-3-3 gene *MdGRF6* negatively regulates salt tolerance. *Front Plant Sci*. 2023. <https://doi.org/10.3389/fpls.2023.1161539>.
  71. Abe M, Kobayashi Y, Yamamoto S, Daimon Y, Yamaguchi A, Ikeda Y, Ichinoki H, Notaguchi M, Goto K, Araki T. FD, a bZIP protein mediating signals from the floral pathway integrator FT at the shoot apex. *Science*. 2005;309(5737):1052–6.
  72. Wigge PA, Kim MC, Jaeger KE, Busch W, Schmid M, Lohmann JU, Weigel D. Integration of spatial and temporal information during floral induction in *Arabidopsis*. *Science*. 2005;309(5737):1056–9.
  73. Beltramino M, Debernardi JM, Ferrel A, Palatnik JF. ARF2 represses expression of plant GRF transcription factors in a complementary mechanism to microRNA miR396. *Plant Physiol*. 2021;185(4):1798–812.

## Publisher's Note

Springer Nature remains neutral with regard to jurisdictional claims in published maps and institutional affiliations.